

Parity dependence of the level densities of ^{53}Cr and ^{55}Cr at high excitation

H. M. Agrawal* and J. B. Garg
State University of New York, Albany, New York 12222

J. A. Harvey
Oak Ridge National Laboratory, Oak Ridge, Tennessee 37831
(Received 16 July 1984)

The neutron total cross sections of ^{52}Cr and ^{54}Cr have been measured in the energy range from a few tens of keV to about 900 keV using a neutron time-of-flight technique and a pulsed electron linear accelerator. The nominal resolution of the measurements was about 0.06 ns/m. The total cross-section data have been analyzed using an R -matrix multilevel multichannel code to determine values of the resonance parameters (E_0 , $g\Gamma_n$, and J^π) and to investigate the parity dependence of the level densities of ^{53}Cr and ^{55}Cr at high excitation. From these analyses we obtain the following values for the average properties of the resonance parameters for s -wave resonances up to about 900 keV and for p -wave resonances up to 600 keV: $D_0=(45\pm 6)$ keV, $S_0(\times 10^4)=(3.0\pm 1.0)$, $D_1=(8.5\pm 0.6)$ keV, $S_1(\times 10^4)=(0.70\pm 0.12)$ for ^{52}Cr ; and $D_0=(60\pm 9)$ keV, $S_0(\times 10^4)=(2.6\pm 0.9)$, $D_1=(9.2\pm 0.5)$ keV, $S_1(\times 10^4)=(0.67\pm 0.11)$ for ^{54}Cr . The distributions of reduced neutron widths for s - and p -wave resonances for each isotope show good agreement with the Porter-Thomas distribution. The values of the Δ_3 statistic for the long-range correlation of s -wave resonances for both ^{52}Cr and ^{54}Cr are found to be in reasonable agreement with the theoretical prediction of Dyson and Mehta. The values for the ratio D_0/D_1 for both nuclides are larger than expected from a $(2J+1)$ level dependence, indicative of a parity dependence of the level densities of ^{53}Cr and ^{55}Cr at high excitation.

I. INTRODUCTION

Precise measurements of neutron total cross sections of the elements used in nuclear reactors supply important data for reactor design and analysis, and they also provide tests of various nuclear reaction and statistical theories. The total cross sections of the isotopes ^{52}Cr and ^{54}Cr are particularly important since stainless steel, which is used as a structural material in fission and fusion reactors, contains natural chromium. Natural chromium largely consists of the isotopes ^{52}Cr (83.76%); however, it also contains ^{54}Cr (2.36%). Because of the low natural abundance of ^{54}Cr , this nuclide has not been studied thoroughly and information on its resonance parameters has been incomplete. Much more data are available on ^{52}Cr , but the very low values for the s - and p -wave neutron strength functions given by measurements for this isotope are inconsistent with optical model calculations. Data on both ^{52}Cr and ^{54}Cr are of particular interest for an understanding of the parameters of the optical model, since these nuclides lie in the immediate neighborhood of the $3S$ giant resonance of the strength function versus mass number plot.

With the availability of an increased neutron energy resolution at the Oak Ridge Electron Linear Accelerator (ORELA) and highly enriched samples, it was expected that measurements of the total cross sections of ^{52}Cr and ^{54}Cr made at ORELA and presented in this paper would result in more complete and more precise sets of data for both nuclides than those reported previously. Moreover, analyses of the resulting high-quality data could lead to a better understanding of neutron interactions with these

nuclides. As described below, the analyses performed included determination of neutron strength functions¹ and investigations of the concept of doorway states² for this mass region. In addition, the predictions of the statistical theories were tested regarding the distributions of level energies³ and reduced neutron widths,⁴ the $(2J+1)$ level density law,⁵ and the dependence of level density on parity.

A. Experimental details

Since the experimental system at ORELA, a high-intensity neutron facility, has been described in an earlier publication,⁶ only the relevant features will be mentioned here. The accelerator was operated at a power of 10 kW

TABLE I. Mass analyses of the $^{52,54}\text{Cr}$ samples used for the present measurements. (Impurity elements $< 0.01\%$.)

Samples (Cr_2O_3)	Isotope	at. %	Precision
^{54}Cr	50	0.01	
	52	99.87	± 0.02
	53	0.12	± 0.02
	54	0.01	
^{54}Cr	50	0.18	± 0.05
	52	3.09	± 0.10
	53	1.33	± 0.10
	54	95.40	± 0.10

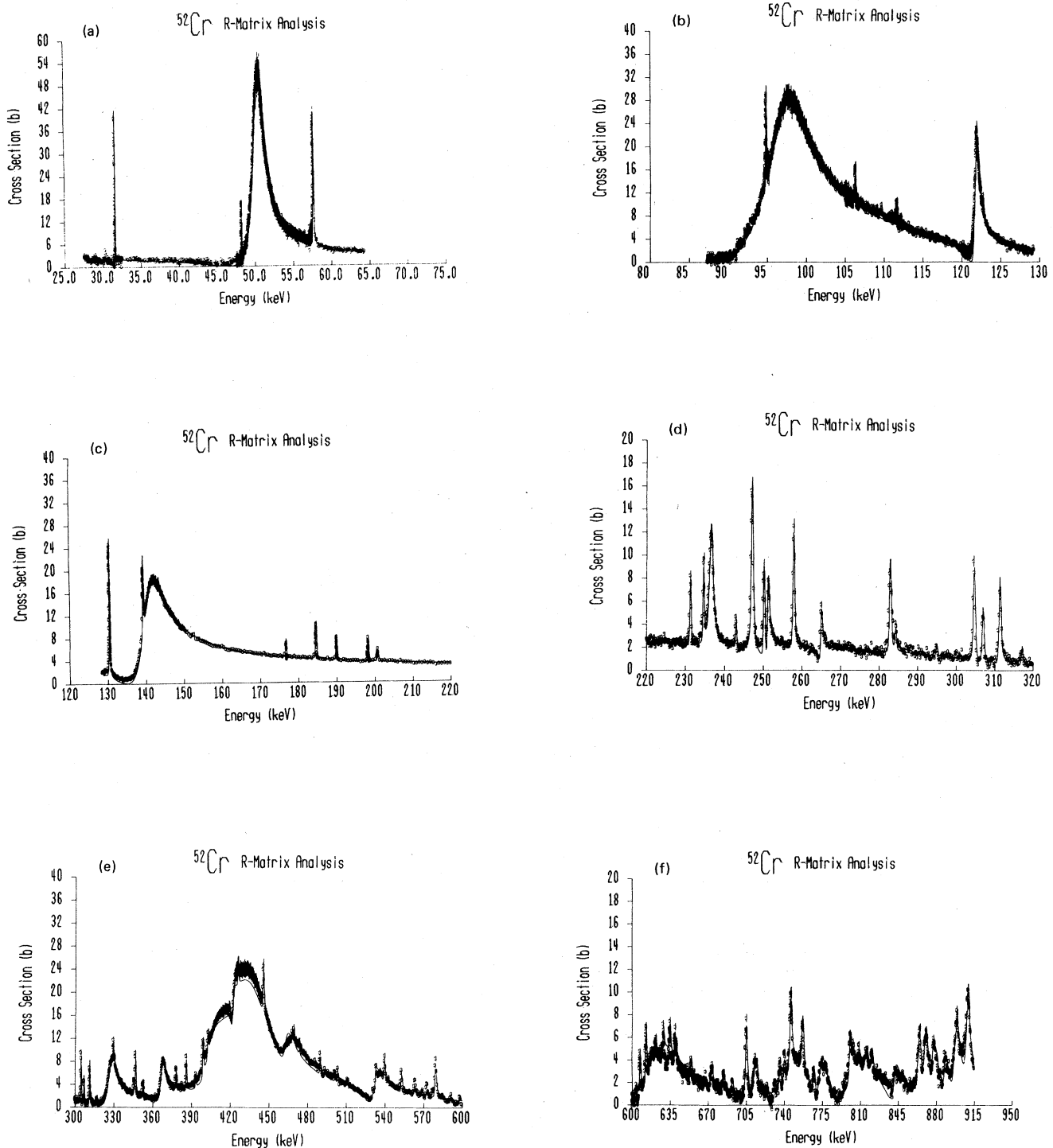


FIG. 1. R-matrix multilevel fit (solid lines) to the total cross-section data (points) for ^{52}Cr in the neutron energy range from 25 to 915 keV.

with a neutron burst width of 5 ns at a repetition rate of 800 Hz. A flight-path length of 78.203 m was used. The neutron detector was an NE-110 fast scintillator mounted on a 127-mm diam RCA 8854 photomultiplier tube.

The samples were Cr_2O_3 enriched to 99.87% in mass 52 and to 95.40% in mass 54, with inverse thicknesses of $1/n = 25.33b/a$ for the ^{52}Cr sample and $1/n = 18.48b/a$ for the ^{54}Cr sample. The sample enrichments are listed in

Table I. The accelerator running time was about one week, and the analyses of the data were carried out over a period of about two years.

B. Data analysis

Neutron total cross sections for ^{52}Cr and ^{54}Cr were determined over the energy range from a few tens of keV

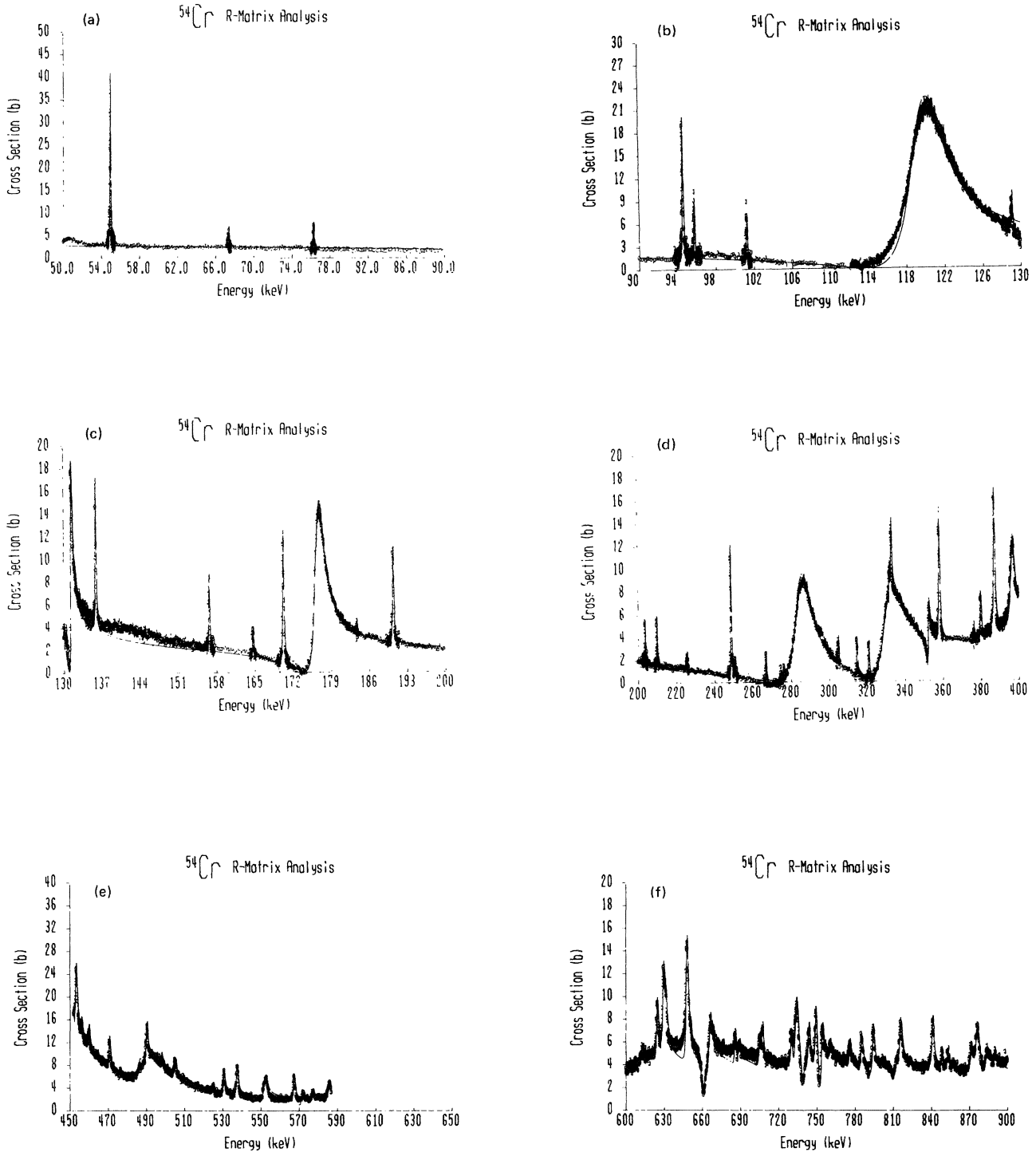


FIG. 2. *R*-matrix multilevel (solid lines) to the total cross-section data (points) for ^{54}Cr from 50 to 900 keV. The difference between the theoretical curve and the data around 98 and 140 keV is due to the contribution from ^{52}Cr *s*-wave resonances.

to 900 keV from the transmission of the neutron beam through the chromium oxide samples. The data obtained both with the open beam and with the samples in the beam were corrected for the dead time of the time digitizer (1104 ns) and for background contributions described earlier.⁶ The resulting cross sections were partially corrected for the oxygen content of the samples by sub-

tracting $1.5 \times [3.6 - (2 \times 10^{-6})E]$ (in eV) b over the full energy range. (This correction is adequate only for energies below 300 keV.)

The partially corrected cross-section data for both isotopes were analyzed with the multilevel multichannel code NewMULTI to determine the resonance energies E_0 , the neutron widths Γ_n , and the J^π of the resonances. Because

TABLE II. Parameters of *s*-wave resonances obtained from an *R*-matrix analysis of ⁵²Cr data.

$E_0 \pm \Delta E_0$ (eV)	$\Gamma_n \pm \Delta \Gamma_n$ (eV)	$E_0 \pm \Delta E_0$ (eV)	$\Gamma_n \pm \Delta \Gamma_n$ (eV)
31 646±8	12±4	421 890±150	1500±80
50 358±15	1810±90	462 820±200	6800±300
96 710±40	7510±150	532 550±200	4800±100
121 810±50	550±30	617 500±200	35 000±3000
140 500±90	5200±500	653 650±300	1000±80
251 130±80	300±20	738 050±300	40 000±3000
264 900±100	145±15	766 400±300	4000±400
326 230±120	7500±300	771 900±400	8000±800
366 340±130	4340±100	798 250±400	30 000±3000
403 060±140	15 000±1000	840 500±400	6000±500

TABLE III. The parameters ($E_0 \pm \Delta E_0$, $g\Gamma_n \pm \Delta g\Gamma_n$, g) of $l \geq 1$ resonances obtained from an *R*-matrix analysis of ⁵²Cr data.

$E_0 \pm \Delta E_0$ (eV)	$g\Gamma_n \pm \Delta g\Gamma_n$ (eV)	g	$E_0 \pm \Delta E_0$ (eV)	$g\Gamma_n \pm \Delta g\Gamma_n$ (eV)	g	$E_0 \pm \Delta E_0$ (eV)	$g\Gamma_n \pm \Delta g\Gamma_n$ (eV)	g
1626±5 ^a	0.072±0.012	2	393 300±90	180±20	1	684 700±200	440±50	2
5270±10 ^a	0.013±0.005	2	399 010±90 ^b	720±40	2	692 400±200	310±30	2
22 940±20 ^a	3.6±1.0	2	402 600±100	320±20	2	705 400±200 ^c	3000±300	3
48 240±4	9±2	1	426 000±110	350±20	1	711 300±200	280±40	1
57 678±5 ^b	85±8	1	445 850±110 ^b	1120±60	2	713 110±200 ^b	1500±130	2
94 861±10	40±6	1	468 480±110	110±15	1	714 710±200 ^b	1200±110	2
106 314±12	21±4	2	469 700±110	90±20	2	719 640±200	230±30	1
109 640±12	6±1	1	473 750±120	58±8	1	724 560±200	90±30	1
111 699±14	9±2	1	489 960±120	340±40	2	731 390±200	150±20	1
130 500±20 ^b	350±80	2	493 620±120	50±5	1	736 160±200 ^b	700±70	2
139 330±20 ^b	440±20	2	501 440±120	60±10	1	740 200±200 ^b	650±70	2
143 330±30	25±5	1	503 710±130	210±20	2	746 950±200 ^b	3000±300	2
176 800±30	18±5	1	511 390±130	36±4	1	756 900±200 ^b	3600±300	2
183 930±30	5±1	1	530 500±140	36±4	1	757 000±200 ^c	200±30	2
184 700±30 ^b	132±12	1	533 000±140	270±30	2	761 500±200	600±60	1
190 010±30	70±7	1	536 340±140	180±20	1	767 100±200	40±5	2
198 300±30	70±8	1	539 690±140 ^b	750±100	2	778 800±200	150±20	1
200 830±30	36±4	1	542 650±140	100±20	1	800 800±000	2400±300	2
231 290±40	164±5	1	552 850±150 ^b	600±60	2	803 760±200	750±80	1
234 650±40	175±10	2	563 160±150	200±20	2	808 840±200	360±60	2
236 570±40 ^b	1010±50	1	569 040±150	44±10	1	815 630±300	480±50	2
242 920±40	45±10	1	572 700±150	200±20	2	817 000±300	240±40	1
247 130±40 ^b	750±20	2	576 900±150	45±5	1	821 000±300 ^b	900±100	2
250 200±40 ^b	275±15	2	579 200±160 ^b	1400±150	2	864 860±300 ^b	2400±300	2
251 400±50 ^b	225±14	2	591 560±160	36±4	1	865 100±300	4000±400	1
257 850±50 ^b	440±20	2	597 890±160	45±5	1	869 230±300	800±150	1
282 900±60 ^b	440±20	2	603 800±160	75±15	1	871 000±300 ^b	8900±900	2
284 280±50	65±7	1	607 600±160	800±80	2	874 320±300	640±110	1
295 040±60	12±2	1	612 960±170 ^b	1500±150	2	877 200±300 ^b	6000±800	2
304 700±60 ^b	480±20	2	616 390±170	180±20	1	880 820±300	2400±500	1
306 950±60 ^b	249±11	2	618 200±170	340±40	1	883 400±300	800±200	1
311 330±60 ^b	410±20	2	621 820±170	340±40	2	888 680±300 ^b	3300±600	2
317 130±60	72±8	1	629 060±180	300±30	2	891 250±300	1200±300	1
329 620±70	117±13	2	634 840±180 ^b	600±60	2	898 000±300 ^b	8500±1000	1
330 500±70	27±3	1	639 520±180 ^b	500±50	2	899 150±300	400±80	1
345 650±70	37±10	1	654 550±180	400±40	2	906 400±300	500±50	1
346 730±70 ^b	550±20	2	667 900±190	160±20	1	909 400±400 ^c	5100±500	3
352 650±70	180±20	2	672 350±190	270±30	1			
378 190±80	220±20	2	674 100±190	450±50	2			
382 680±80	36±4	1	683 400±190	270±30	1			
385 960±80	510±30	2	686 710±190	130±30	1			

^aTaken from Brookhaven National Laboratory Report BNL-325, 1981.^bSpins determined with certainty; spins for other resonances are preferred or assumed.^cFitted as *d*-wave resonances.

TABLE IV. Parameters of s -wave resonances obtained from an R -matrix analysis of ^{54}Cr data.

$E_0 \pm \Delta E_0$ (eV)	$\Gamma_n \pm \Delta \Gamma_n$ (eV)	$E_0 \pm \Delta E_0$ (eV)	$\Gamma_n \pm \Delta \Gamma_n$ (eV)
23 050 ± 10	600 ± 50	552 350 ± 200	1800 ± 300
119 300 ± 40	4100 ± 200	595 000 ± 200	80 000 ± 10 000
131 350 ± 50	300 ± 30	662 380 ± 300	10 000 ± 2000
176 400 ± 60	1950 ± 110	738 650 ± 300	2000 ± 200
283 370 ± 80	10 700 ± 900	753 060 ± 300	4500 ± 400
329 800 ± 100	11 600 ± 1000	790 500 ± 300	1100 ± 100
352 300 ± 120	500 ± 60	809 600 ± 400	1000 ± 100
485 980 ± 200	12 000 ± 1100		

of strong interference effects between resonances, the multilevel approach was necessary to obtain proper fits to the data. The cross-section fitting was done on a UNIVAC 1100 computer at the State University of New York at Albany.

For the analyses above 300 keV, contributions from the well-known strong resonances in oxygen at 0.433 and 1.00 MeV were calculated from the parameters given in BNL-325 (1981) (Ref. 7) and were held fixed. The parameters of the chromium resonances near these oxygen resonances cannot be determined quite as accurately.

The experimental total cross-section data (points) and the theoretical fits (solid lines) for ^{52}Cr from 25 to 915 keV are shown in Figs. 1(a)–(f), and those for ^{54}Cr from 50 to 900 keV are shown in Figs. 2(a)–(f). The theoretical fits to the data are excellent for both nuclides for the full energy range except for ^{54}Cr near 98 and 140 keV, where the experimental data are higher because of the contributions from broad ^{52}Cr s -wave resonances (3.09 at. % ^{54}Cr in the sample).

The final values of E_0 and $g\Gamma_n$ for s -wave resonances for ^{52}Cr are given in Table II and values of E_0 , $g\Gamma_n$, and $g(J + \frac{1}{2})$ for $l \geq 1$ are given in Table III. Corresponding quantities for ^{54}Cr are presented in Tables IV and V. A discussion of the uncertainties in the E_0 and $g\Gamma_n$ values has been given previously⁸ and, thus, will not be repeated here.

II. DISCUSSION OF RESULTS FOR ^{52}Cr

A. s -wave resonances (^{52}Cr)

The parameters of the 20 s -wave resonances determined from our transmission measurements for ^{52}Cr (see Table II) were compared with the values recommended by Mughabghab *et al.* in BNL-325 (Ref. 7), which for energies below about 250 keV are based mainly on data reported by Stieglitz *et al.*,⁹ Beer and Spencer,¹⁰ and Allen *et al.*,¹¹ and for energies above 250 keV on data reported by Bowman *et al.*¹² The data of Stieglitz *et al.* and Beer and Spencer were obtained from capture and transmission measurements having overall resolutions of 0.6 ns/m, which were about ten times poorer than that of our measurements. The data of Bowman *et al.*¹² were from transmission measurements with a 3-MeV Van de Graaff with an energy homogenizer; the overall resolution of their measurements was about 500 eV, which is compar-

able to the resolution of our measurements only at the maximum energy of about 1 MeV and is much worse at lower energies.

Like our data, the data of Allen *et al.*¹¹ were obtained at ORELA, but the measurements were capture measurements and the flight-path length was 40 m vs about 80 m in our measurements. The capture measurements had a greater sensitivity for detecting narrow resonances than did our transmission measurements. For those cases in which a narrow resonance not seen by us was observed in the capture measurements, we can estimate an upper limit of the neutron width of the resonance on the basis of our detection sensitivity.

In comparing our data with the results of others, we found that Mughabghab *et al.*⁷ listed an s -wave resonance at 118.2 keV that was not observed in our data. This resonance, initially reported by Beer and Spencer,¹⁰ also was not observed by Allen *et al.* and is believed to be spurious or due to a broad resonance in ^{54}Cr contamination.

We observed broad resonances at 235.8 and near 628.5 keV, but since the resonances are not asymmetrical, they cannot be s -wave resonances, in contradiction to the $l = 0$ assignment by Bowman *et al.*¹² that was recommended.⁷ We did find s -wave resonances at 251.1 and 264.9 keV that were not observed by Bowman *et al.*

Overall, the resonance energies measured by us are consistently higher by about 0.5% than the recommended values.⁷ The neutron widths differ by about 10% up to about 350 keV, but differ much more at higher energies.

B. Average level spacing for s -wave resonances (^{52}Cr)

Figure 3 shows a plot of the number of ^{52}Cr s -wave resonances observed in our measurements versus neutron energy. At 500 keV, the average neutron width for s -wave resonances is 9 keV, which is much larger than the instrumental resolution width of ~ 0.6 keV even at this neutron energy; consequently, the possibility that an s -wave resonance has been missed is quite small even at the maximum neutron energy of about 900 keV. From the slope of the straight line drawn through the plot in Fig. 3 we have determined a value of 45 ± 6 keV for the s -wave average level spacing D_0 . In this determination we have ignored the small exponential increase of level density with energy which partially compensates for small resonances missed at high energies. The fact that the data can be fit-

TABLE V. The parameters ($E_0 \pm \Delta E_0$, $g\Gamma_n \pm \Delta g\Gamma_n$, g) of $l \geq 1$ resonance obtained from the R -matrix analysis of ^{54}Cr data.

$E_0 \pm \Delta E_0$ (eV)	$g\Gamma_n \pm \Delta g\Gamma_n$ (eV)	g	$E_0 \pm \Delta E_0$ (eV)	$g\Gamma_n \pm \Delta g\Gamma_n$ (eV)	g
10 290±10 ^a	0.400	1	505 100±130 ^b	750±100	1
14 443±5	1.3±0.2	1	525 120±130	150±30	1
14 825±6	0.42±0.10	1	530 670±140 ^b	800±80	2
19 210±8	0.60±0.14	1	537 590±140 ^b	1050±150	2
51 130±5	0.40±0.10	2	551 670±150	450±50	1
54 912±5 ^b	59±4	1	567 450±150 ^b	900±100	2
67 379±6	2.6±0.5	1	572 250±150	250±30	1
76 292±8	6.5±0.5	1	577 350±160	250±50	1
94 602±10 ^b	86±9	1	585 970±160 ^b	800±150	1
95 776±10	24±5	1	612 550±170	40±10	1
101 260±12	21±5	1	614 100±170	200±20	1
129 060±20	16±4	1	621 130±170	150±30	1
135 900±20 ^b	129±15	1	624 000±170	400±40	1
156 600±20	68±7	1	625 100±180 ^b	1600±200	2
164 700±20	19±5	1	627 600±180	250±50	1
170 200±30 ^b	180±20	1	629 300±180 ^b	3200±400	2
183 800±30	6±2	1	631 100±180	2800±400	1
190 400±30	141±15	1	647 900±180 ^c	4000±500	2
203 640±30	86±9	1	648 020±180 ^b	1000±200	2
209 810±30	97±10	1	651 100±190	200±30	1
225 570±40	32±12	1	666 380±190 ^b	3600±700	1
248 600±40 ^b	500±50	2	685 800±200	1000±100	2
249 630±40	17±2	1	689 000±200	700±80	1
250 680±50	26±10	1	704 910±200 ^b	1100±100	1
266 840±50	98±9	1	707 400±200 ^b	900±90	2
274 560±50	9±2	1	730 160±200 ^b	1100±110	2
276 250±50	15±4	1	732 900±200	600±80	1
304 920±60	106±10	1	734 200±200 ^b	3000±400	2
314 700±60	175±15	1	743 800±200 ^b	2000±300	2
320 870±60	180±20	1	749 000±200 ^b	2100±400	2
332 290±70	100±30	1	754 150±200 ^b	2200±500	2
333 170±70	300±50	1	760 680±200	630±120	1
358 310±80 ^b	501±100	2	775 850±200	990±140	1
376 480±80	70±20	1	785 080±300 ^b	1000±110	2
380 050±80	300±60	1	794 000±300 ^b	1200±300	2
385 930±90	100±30	1	812 720±300	700±70	1
387 270±90 ^b	1000±300	2	815 700±300 ^b	2500±300	2
396 900±90 ^b	2000±400	1	838 240±300	390±50	1
430 860±100	1800±400	1	840 580±300 ^b	1400±200	2
441 560±100 ^b	3000±500	2	840 810±300	450±50	1
453 350±110 ^b	2400±600	2	848 190±300	430±50	1
456 250±110	400±50	1	853 110±300	410±40	1
458 000±110	120±30	1	871 530±300 ^b	2200±200	1
460 000±110	600±100	1	875 800±300 ^b	2300±200	2
470 730±110 ^b	900±90	2	883 460±300 ^b	900±90	2
486 460±120	75±15	1	885 820±300	380±30	1
490 320±120 ^b	950±150	2	890 100±300	400±40	1
498 200±130	200±50	1			

^aTaken from Brookhaven National Laboratory Report BNL-325, 1981.

^bSpins determined with certainty; spins for other resonances are preferred or assumed.

^cFitted as d -wave resonance.

ted by a straight line up to the highest neutron energy may also be due to the uncertainty associated with the small number of observed resonances (as given in Table VI).

The statistic Δ_3 of Dyson and Mehta³ is quite sensitive to the strategic location and the lack of levels in a pure se-

quence of levels. Dyson and Mehta have calculated the expected behavior of Δ_3 and its standard deviation for a single population of n levels of the same J^π . They find that

$$\langle \Delta_3 \rangle = 1/\pi^2 [\ln(n) - 0.0687]$$

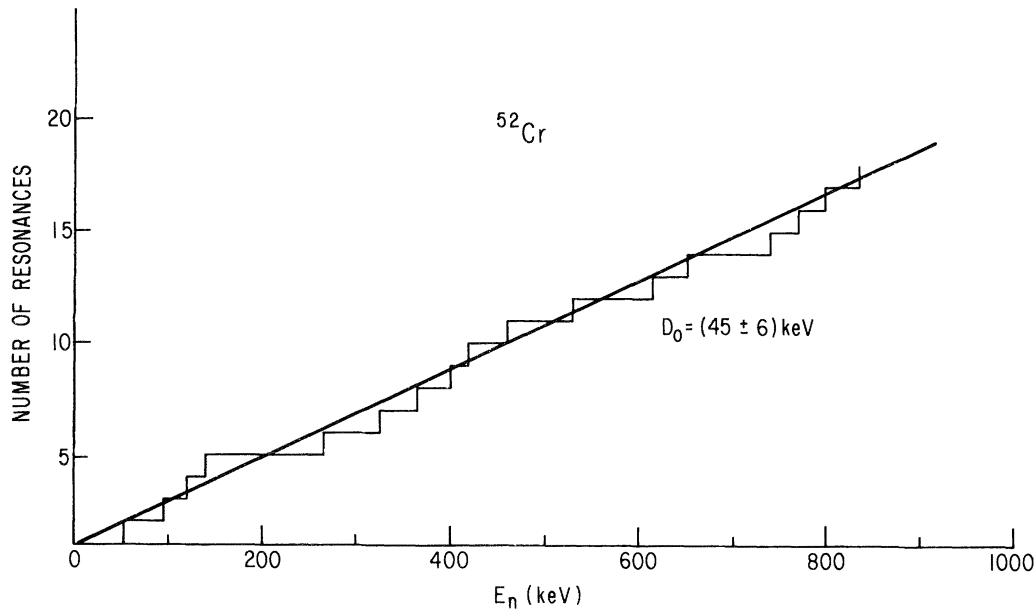


FIG. 3. Number of ^{52}Cr s -wave resonances versus neutron energy. The slope of the straight line passing through the points gives an estimate of the mean level spacing.

with a standard deviation of 0.11. We determined values of Δ_3 from our data for s -wave resonances in four energy intervals (see Table VI). Our experimental value of 0.27 for 13 resonances up to 600 keV is in excellent agreement with the theoretical prediction of 0.25 ± 0.11 , and the values obtained for the other intervals are also in good agreement with the corresponding theoretical values.

C. Distribution of reduced neutron widths for s -wave resonances (^{52}Cr)

It is now well established that the Porter-Thomas single-channel distribution law,⁴ which is the outcome of extreme configuration mixing based on the compound nucleus model of neutron interaction, should apply to a single-level population over an energy interval that is not affected by intermediate structure fluctuations. Even though we had some evidence of intermediate structure, we compared the distribution of our data with the Porter-Thomas distribution, which gives the probability distribu-

tion of the square roots of reduced neutron widths (y) as follows:

$$P(y)dy = (2/\pi)^{1/2} \exp[-y^2/2] dy,$$

where $y = (\Gamma_n^i / \langle \Gamma_n^i \rangle)^{1/2}$. The reduced neutron width of a resonance, Γ_n^i , equals $kR\Gamma_n/P_1\sqrt{E_0}$, where R is the nuclear radius. The distribution of reduced neutron width amplitudes for the 20 s -wave resonances up to about 900 keV is shown in Fig. 4, together with the Porter-Thomas theoretical curve. The histogram shows good agreement with theory.

A more meaningful quantity is the numerical value of ν , the number of degrees of freedom of a chi-squared distribution. We have calculated the value of ν by the maximum likelihood method (as discussed by Porter and Thomas), and found it to be 1.4 ± 0.4 for the 20 resonances up to 900 keV. We also used a Monte Carlo program (GNEW) based on the maximum likelihood method of Beer¹³ to determine the value of ν and obtained a value of

TABLE VI. The number of s -wave resonances, average level spacing, the Δ_3 values (experiment and theory) for ^{52}Cr as a function of the energy interval.

Energy range (keV)	No. of resonances	Average level spacing, D_0 (keV)	Δ_3 experiment	Δ_3 theory
0–200	5	40 ± 6	0.14	0.15
0–400	9	45 ± 7	0.29	0.22
0–600	13	46 ± 7	0.27	0.25
0–800	19	47 ± 7	0.39	0.29

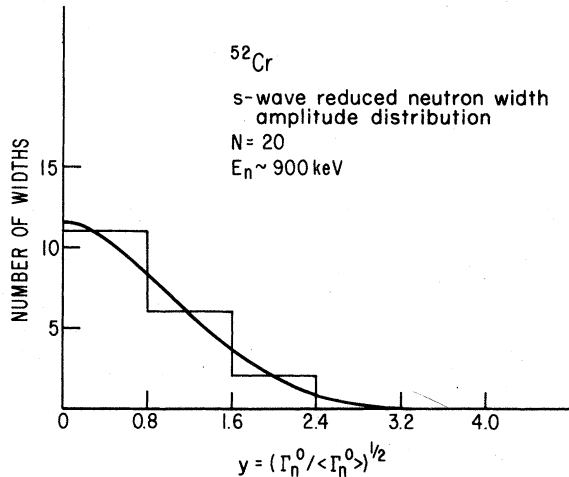


FIG. 4. Distribution of reduced neutron width amplitudes for ^{52}Cr s -wave resonances. The solid curve is the theoretical Porter-Thomas distribution.

1.3 ± 0.4 . These values are in good agreement with the expected value of 1.0 for a Porter-Thomas distribution.

D. s -wave neutron strength function (^{52}Cr)

The sum of Γ_n^0 for the ^{52}Cr s -wave resonances versus neutron energy is plotted in Fig. 5. We see that the data from 0 to 600 keV can be fitted by a straight line with a much smaller slope than those from 600 to 900 keV. This indicates different values of the s -wave neutron strength function, S_0 , for the two energy regions. This change is indicative of the presence of an intermediate structure; however, theoretical calculations would be needed to establish this interpretation. An average value of $S_0 (\times 10^4)$ of 3.0 ± 1.0 is obtained over the entire region up to 900 keV. A summary of values of the s -wave strength function in various energy intervals is given in Table VII.

E. p -wave resonances (^{52}Cr)

As shown in Table III, we determined 114 ^{52}Cr p -wave resonances from our measurements. In general, our p -wave resonance parameters are in fair agreement with the values reported in BNL-325.⁷ However, since the resolution of our measurements was much better than the measurements on which the BNL-325 values were based (Stieglitz *et al.*,⁹ Beer and Spencer,¹⁰ Allen *et al.*,¹¹ and Bowman *et al.*¹²), we observed many more p -wave resonances and have been able to determine more accurate

TABLE VII. s -wave neutron strength function values for ^{52}Cr in different energy intervals.

Energy range (keV)	$S_0 (\times 10^4)$
0–600	2.2 ± 0.8
600–900	5.8 ± 3.1
0–900	3.0 ± 1.0

values for $g\Gamma_n$. For example, in the two intervals from 100 to 200 keV and 200 to 300 keV, we observed 11 and 12 p -wave resonances, respectively, whereas Beer and Spencer observed only five and six resonances. Up to about 280 keV, we observed a total of 26 $l > 0$ resonances, whereas Beer and Spencer observed only 19 $l > 0$ resonances, including five not seen by us (at 27.6, 34.0, 113.0, 153.3, and 165.3 keV). Over the energy interval from 400 to 600 keV, we observed 24 p -wave resonances, whereas Bowman *et al.*¹² found only six resonances; however, the resolution of the measurements of Bowman *et al.*¹² was too poor for their results to be reliable.

With their greater sensitivity for observing resonances with very small neutron widths, Allen *et al.* found a large number of very narrow resonances in the energy interval from 0 to 250 keV which they interpreted as $l > 0$ resonances. On the basis of our own investigation of the reduced neutron width distribution and of level density, we now believe that most of these narrow resonances are d -wave resonances.

F. Average level spacing for p -wave resonances (^{52}Cr)

A plot of the number of ^{52}Cr p -wave resonances versus neutron energy is given in Fig. 6. The departure from linearity above 600 keV is probably due to the expected increase of level density at higher energy rather than to the inclusion of some d -wave resonances. A p -wave average level spacing, D_1 , of 9.0 ± 0.7 keV is found from the inverse slope of the straight line up to about 600 keV. However, as discussed in the following section, we estimate that we have missed about four p -wave resonances, which, if present, would give a revised value for D_1 of 8.5 ± 0.6 keV.

In order to further investigate the l assignments, we estimated conditional probabilities based upon Bayes's theorem, in spite of the fact that the use of this theorem for assigning parities of resonances has been questioned.¹⁴ The probability that a resonance is formed by d -wave neutrons is given by¹⁵

$$P(d \text{ wave}) = \left[1 + \frac{3}{5} \left(\frac{S_2 P_2}{S_1 P_1} \right)^{1/2} \exp \left[\frac{g\Gamma_n}{6D_1 \sqrt{E_n} \text{ (eV)}} \left(\frac{1}{P_2 S_2} - \frac{1}{P_1 S_1} \right) \right] \right]^{-1}$$

where the symbols have the same meanings as discussed in Ref. 15. For these calculations, the values of S_1 and S_2 were taken to be 0.75×10^{-4} and 0.25×10^{-4} , respectively, and the nuclear radius R was taken to be 5.0 fm.

We found that the d -wave probability for about 8% of the resonances is larger than 50%. However, if these narrow resonances were indeed d -wave resonances, there would be an inconsistency with the distribution of the p -wave re-

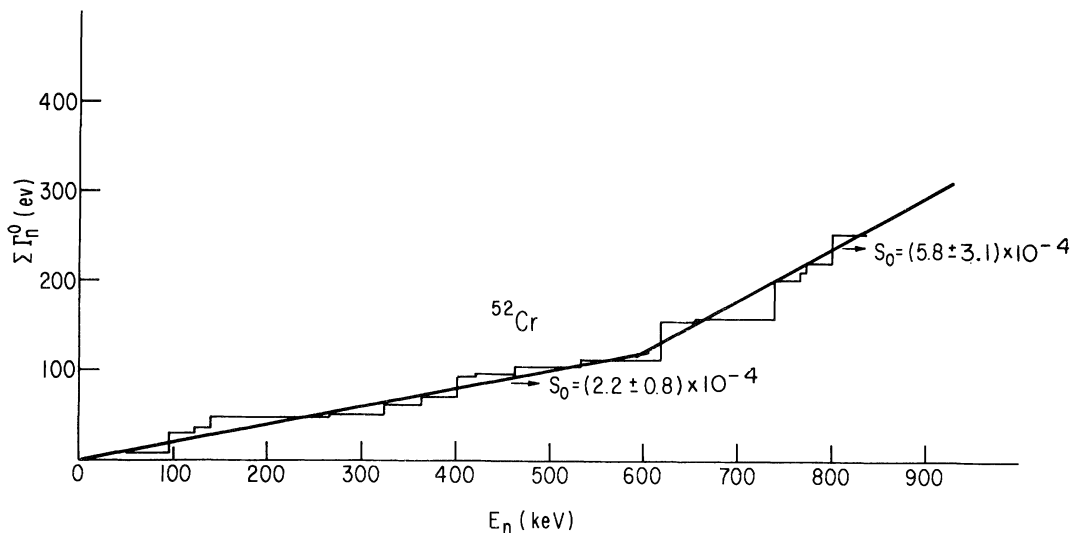


FIG. 5. Sum of reduced neutron widths for ^{52}Cr s-wave resonances versus neutron energy.

duced neutron widths discussed in the following section. Therefore, we have kept these resonances in the p -wave level sequence.

G. Distribution of reduced neutron widths for p -wave resonances (^{52}Cr)

In our measurements, we obtained values of $g\Gamma_n^1$. Since the reduced neutron widths depend on neutron penetrabilities, it is essential to specify the nuclear radius, and we have chosen a value of 5 fm. A comparison of the distribution of the 24 reduced neutron widths which we ob-

served up to 250 keV with the Porter-Thomas distribution⁴ showed that we had missed about four of the narrowest widths. However, Allen *et al.*¹¹ observed 42 $l \geq 1$ resonances in this energy interval. On combining their data with ours, we found an excess of 14 of the narrowest widths above the number expected from the Porter-Thomas distribution. We believe that these 14 narrow resonances are most likely d -wave resonances. Hence, we propose that only 28 resonances should be p -wave resonances, four of which were missed in our measurements.

A plot of the reduced neutron widths of the 68 p -wave resonances observed by us up to 600 keV is shown in Fig.

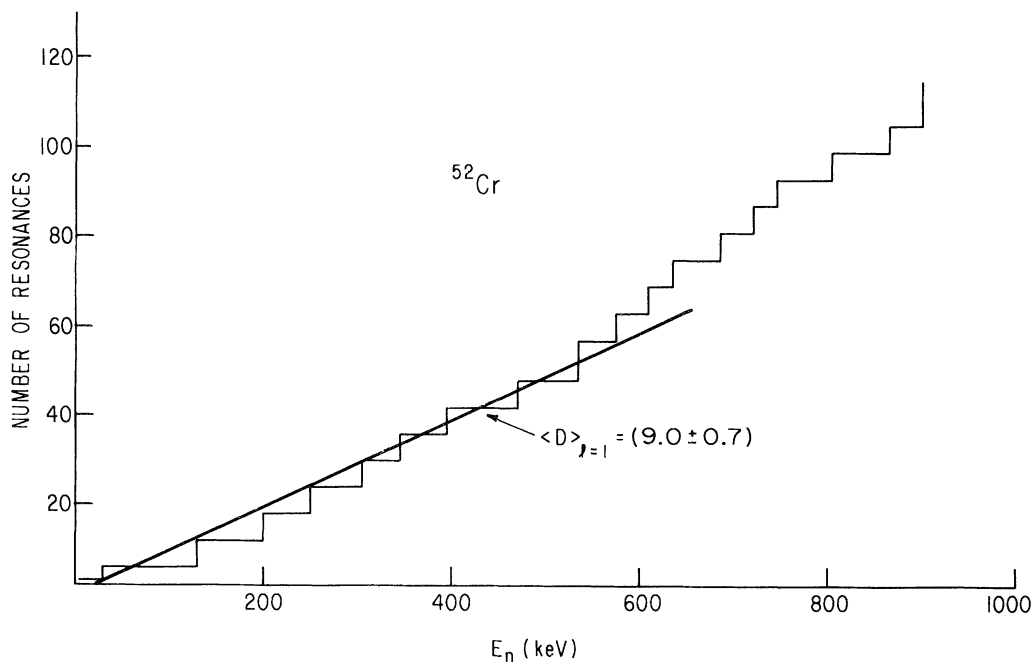


FIG. 6. Number of ^{52}Cr p -wave resonances versus neutron energy. The reduced widths are calculated using a nuclear radius of 5.0 fm.

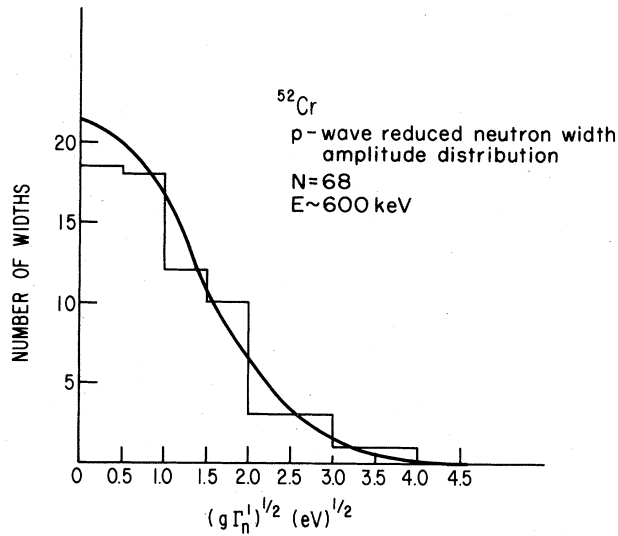


FIG. 7. Distribution of reduced neutron width amplitudes for ^{52}Cr p -wave resonances. The solid curve is the theoretical Porter-Thomas distribution.

7. This plot shows a lack of about four of the narrowest widths, which is again consistent with the data up to 250 keV and also implies that we did not miss any $l=1$ resonances above this energy. A Monte Carlo analysis gives a value of $\nu=1.45\pm 0.30$ for this set of p -wave reduced widths up to 600 keV. This value of ν , which is a little larger than the expected value of 1.0, supports the fact that we did not observe a few of the narrowest widths up to ~ 600 keV.

H. p -wave neutron strength function (^{52}Cr)

The average neutron strength function for a given l over the energy interval ΔE is given as

$$S_l = \sum g_J \Gamma_n^l / (2l+1) \Delta E,$$

where the symbols have the same meanings as discussed previously.⁷ The sum of $g_J \Gamma_n^l / (2l+1)$ vs neutron energy has been plotted in Fig. 8 in order to observe any large fluctuation that could be a manifestation of intermediate structure. We have plotted the sum of $g_J \Gamma_n^l / (2l+1)$ rather than the sum of Γ_n^l for each J separately since many of the J assignments for these resonances are not certain. Up to 800 keV the data can be fitted by a straight line whose slope corresponds to a p -wave neutron strength function, $S_1 (\times 10^4)$, of 0.70 ± 0.12 for the energy region from 0 to 600 keV. However, the data above 800 keV indicate a doorway state in this energy region. From Fig. 8 we determine average values of $S_1 (\times 10^4)$ from 0.70 ± 0.09 up to about 800 keV and 0.95 ± 0.10 up to 900 keV.

III. DISCUSSION OF RESULTS FOR ^{54}Cr

A. s -wave resonances (^{54}Cr)

Table IV shows that we obtained 15 s -wave resonances for ^{54}Cr for neutron energies up to 900 keV. Previous measurements for the ^{54}Cr isotope have been reported by Farrell *et al.*¹⁶ up to 400 keV, by Stieglitz *et al.*⁹ up to 355 keV, and by Allen *et al.*¹¹ up to 285 keV. The same considerations discussed above for the case of ^{52}Cr apply to the quality of the data of these investigators.

Farrell *et al.*¹⁶ used the ^{54}Cr sample in the form of

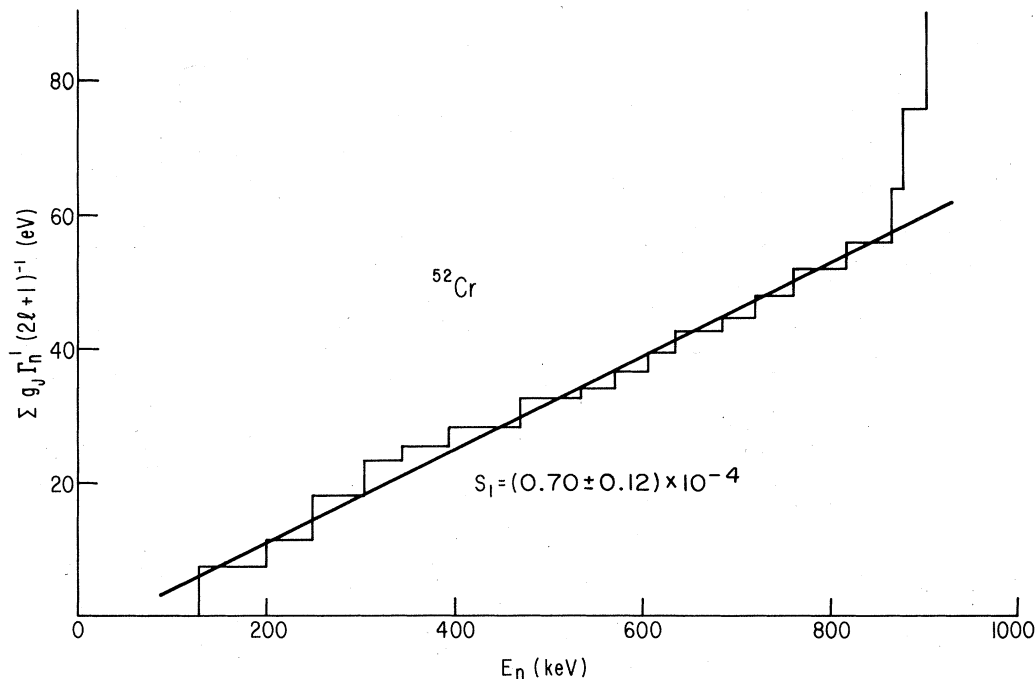


FIG. 8. Sum of reduced neutron widths for ^{52}Cr p -wave resonances versus neutron energy.

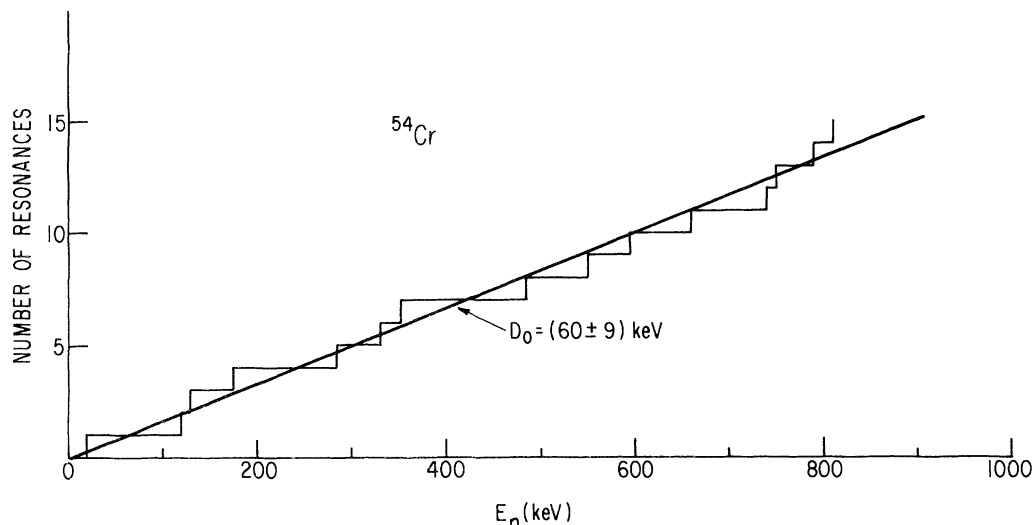


FIG. 9. Number of ^{54}Cr s -wave resonances versus neutron energy.

Cr_2O_3 with 90.6% enrichment in ^{54}Cr . Again, the resolution of their measurements was much poorer than ours below 400 keV. We believe that the resonances they observed at 290.5, 300.5, 342, 355.5, and 393.5 keV are either spurious or due to other isotopes of chromium, since these resonances were not observed in the present measurements made with a more highly (95.4%) enriched sample.

Stieglitz *et al.*⁹ observed six s -wave resonances up to 355 keV, whereas we found seven. Allen *et al.*¹¹ reported a doublet around 280 keV. We observed a single s -wave resonance at 283.4 keV. Mughabghab *et al.*⁷ recommended a doublet around 327 keV, probably on the basis of different energies quoted by Farrell *et al.*¹⁶ and by Stieglitz *et al.*⁹ for the same resonance, but we did not see a doublet in our data. Our data can be fitted by a single resonance at 329.8 keV with $g\Gamma_n = 11.6$ keV.

B. Average level spacing and distribution of reduced neutron widths for s -wave resonances (^{54}Cr)

From the plot of the number of ^{54}Cr s -wave resonances versus energy, shown in Fig. 9, we obtain a value for D_0 of 60 ± 9 keV. The experimental value obtained for the Δ_3 statistic up to 900 keV was 0.34, which is in excellent agreement with the theoretical value of 0.26 ± 0.11 .

The distribution of the square roots of the reduced neutron widths for the 15 s -wave resonances is in very good agreement with the Porter-Thomas distribution, as shown in Fig. 10. The maximum likelihood analysis⁴ of this set of s -wave reduced neutron widths gives a value for ν of 1.23 ± 0.30 , while a Monte Carlo analysis gives a value of 1.10 ± 0.30 . These values of ν are in excellent agreement with the expected value of 1.0.

C. s -wave neutron strength function (^{54}Cr)

The sum of Γ_n^0 for the ^{54}Cr s -wave resonances is plotted as a function of neutron energy in Fig. 11. In the absence

of an intermediate structure, the fit should be linear with the slope being a measure of the s -wave strength function over the entire energy interval. The increased strength at about 300 keV is more likely to be statistical rather than an indication of a doorway state. We have found a value for $S_0(\times 10^4)$ of 1.8 ± 0.9 up to 350 keV, which is in agreement with the value reported by Stieglitz *et al.*⁹ The large step at 595 keV is indicative of intermediate structure. As a result of this large resonance at 595 keV, the value of $S_0(\times 10^4)$ up to 900 keV is 2.6 ± 0.9 .

D. p -wave resonances (^{54}Cr)

Very little information has previously been available about p -wave resonances in ^{54}Cr . We have observed about 35 resonances up to 396 keV (see Table V), whereas Mughabghab *et al.*⁷ recommended only 15 levels on the basis of earlier measurements made by Farrell *et al.*¹⁶

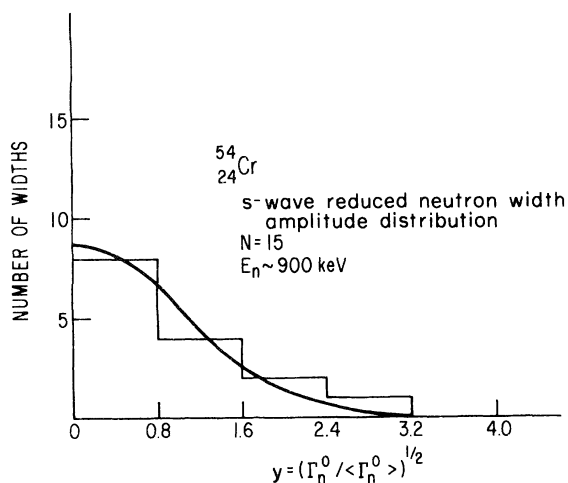


FIG. 10. Distribution of reduced neutron width amplitudes for s -wave resonances of $^{54}\text{Cr} + n$ observed up to about 900 keV. The curve is the Porter-Thomas distribution.

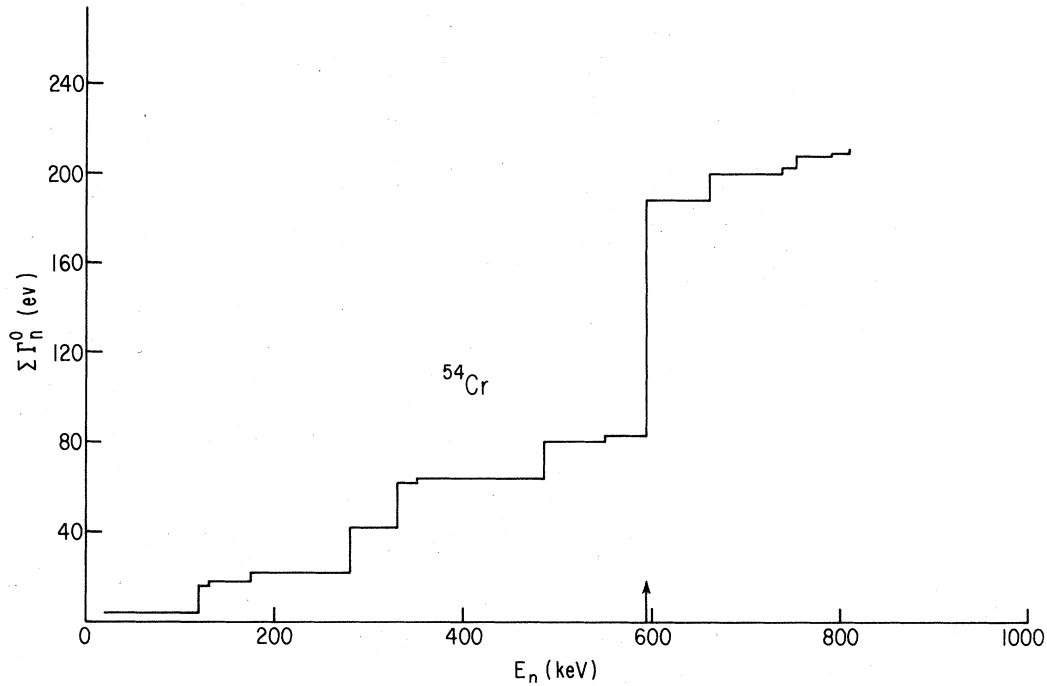


FIG. 11. Sum of reduced neutron widths for ^{54}Cr s -wave resonances versus neutron energy.

Stieglitz *et al.*,⁹ and Allen *et al.*¹¹ This comparison illustrates the importance and need of high-resolution experiments. Our p -wave level sequence consists of all previously reported $l > 0$ resonances in the above energy interval except one at 285 keV, which was observed by Farrell *et al.* but not by us. This resonance may be due to contamination of the samples used in the experiments of Farrell *et al.*¹⁶

E. Average level spacing for p -wave resonances (^{54}Cr)

A plot of the number of ^{54}Cr p -wave resonances versus neutron energy is shown in Fig. 12. An average p -wave level spacing, D_1 , of 10.0 ± 0.6 keV is found from the inverse slope of the straight line up to about 600 keV. However, about five p -wave resonances may not have been observed, as pointed out in the following section. When we

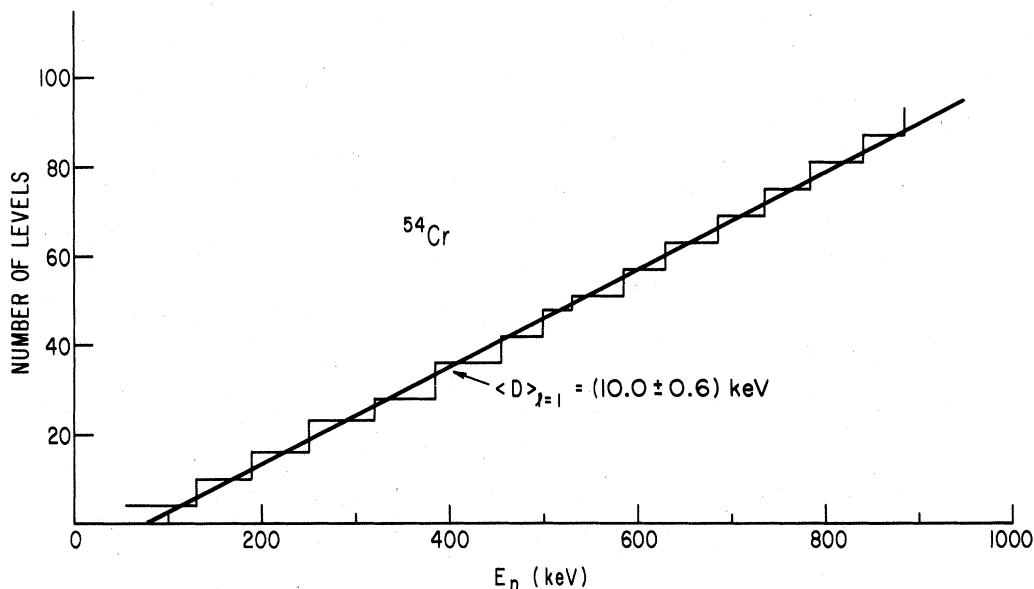


FIG. 12. Number of ^{54}Cr p -wave resonances versus neutron energy.

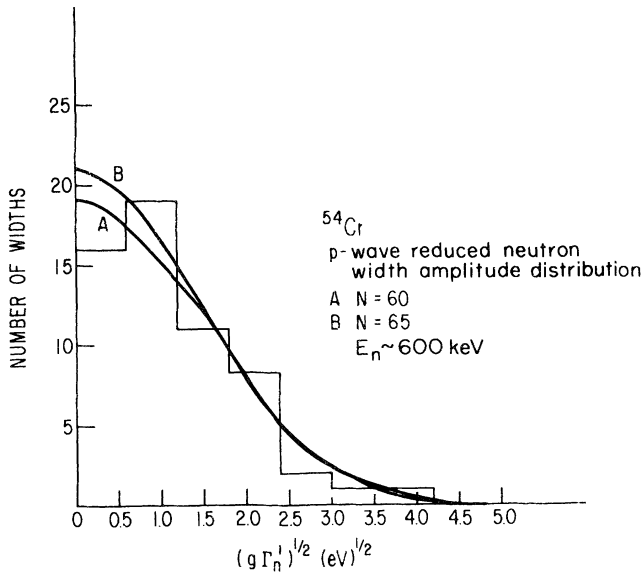


FIG. 13. Distribution of reduced neutron width amplitudes for ^{54}Cr p -wave resonances. A and B are Porter-Thomas distribution curves normalized for 60 and 65 resonances.

include these missing resonances, we obtain a revised value for D_1 of 9.2 ± 0.5 keV.

F. Determination of reduced neutron widths for p -wave resonances (^{54}Cr)

Figure 13 shows a plot of the experimental distribution of the square roots of 60 ^{54}Cr p -wave reduced neutron widths observed up to $E_n \sim 600$ keV. A comparison of

TABLE VIII. p -wave strength function values for ^{54}Cr in different neutron energy intervals. A value of the nuclear radius $R = 5.0$ fm was used for calculating p -wave reduced neutron widths.

E_n (keV)	S_1 ($\times 10^4$)
0–350	0.37 ± 0.08
350–900	1.30 ± 0.21
0–600	0.67 ± 0.12
0–900	0.87 ± 0.11

this distribution with the Porter-Thomas distribution shown by curve A shows that there is a lack of a few narrow widths in the data. This effect is the consequence of our inability to observe very narrow resonances in the transmission measurements. Curve B , which is normalized to 65 resonances, shows good agreement with the experimental histogram for values of $g\Gamma_n^1 > 0.25$ eV. Thus, we may have missed five p -wave resonances.

G. p -wave neutron strength function (^{54}Cr)

A plot of the sum of the reduced neutron widths versus neutron energy up to 900 keV for the p -wave resonances in ^{54}Cr is shown in Fig. 14. We see that the data from 0 to about 350 keV lie on one straight line, while those from 350 to 900 keV lie on another straight line with a different slope, giving rise to different values of S_1 for the two energy regions. This change at 350 keV may be due to the presence of a doorway state above this energy. The two values of S_1 within and outside the doorway are given in Table VIII. Average values for $S_1 (\times 10^4)$ of 0.67 ± 0.12

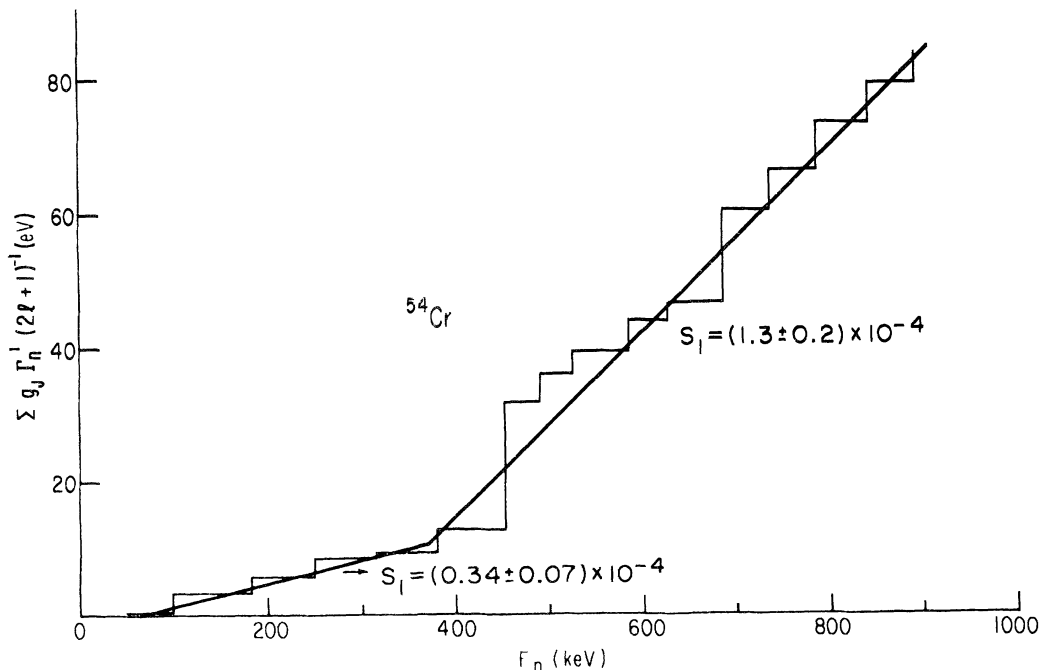


FIG. 14. Sum of reduced neutron widths for ^{54}Cr p -wave resonances versus neutron energy.

and 0.87 ± 0.11 are obtained for neutron energies up to ~ 600 and 900 keV, respectively.

IV. MASS DEPENDENCE

OF *s*-WAVE NEUTRON STRENGTH FUNCTION

Using the doorway concept of Block and Feshbach,² Muller and Rohr¹⁷ studied the fluctuations of the then available experimental neutron strength function values in the $3S$ giant resonance region around the gross curve calculated from the optical model. They explained these fluctuations as variations of the density of doorway states near the binding energy, the density of the states being calculated on the basis of the shell model. They then related the ratio of the average neutron width, $\langle \Gamma \rangle$, to the average spacing, D , in the compound system to the corresponding average values of the doorway system by the following equation given in the Block-Feshbach paper:²

$$\langle \Gamma \rangle / D = \bar{\Gamma} \uparrow / D_d = \sum \Gamma \uparrow / \Delta E = \omega \bar{\Gamma} \uparrow = \omega S_{\text{opt}} \bar{a},$$

where $\Gamma \uparrow$ is the escape width of the doorway state, D_d is the average level spacing of the doorway states, ω is the average number of doorway states per energy unit, S_{opt} is the optical model strength function, and \bar{a} is the residual matrix element. The fluctuations of the strength function enter via the values of ω .

Muller and Rohr presented their results in both tabular and graphical form (see Table VII and Fig. 5 in their paper¹⁷). The calculated values of the *s*-wave neutron strength function, over an averaging energy interval of 1.0 MeV, were 2.3 and 0.9 for ^{52}Cr and ^{54}Cr , respectively, which are in excellent agreement with our experimental values of 2.2 ± 0.8 and 1.5 ± 0.6 at energies below the presence of intermediate structure. This agreement thus provides further confidence in the concept of the doorway picture to explain variations of strength functions among different isotopes of the same element.

V. LEVEL DENSITY AT HIGH EXCITATION ENERGIES

The level density of the compound nucleus at high excitation energies has been a subject to study for many years. Two important features are now well known: (1) that the level density, ρ , in general increases exponentially with the excitation energy, U , and (2) that the level density at a given excitation energy depends on the angular momenta, J , by the following expression:

$$\rho_J(U) = \rho_0(U^*) (2J+1) \exp \frac{-(J + \frac{1}{2})^2}{2\sigma^2},$$

where σ is the spin cutoff parameter which is related to the moment of inertia of the nucleus.

For the $^{52,54}\text{Cr}$ nuclides, *s*-wave neutrons populate resonances with unique spin and parity ($\frac{1}{2}^+$), whereas *p*-wave neutrons give rise to states with $J = \frac{1}{2}$ and $\frac{3}{2}$ and negative parity. If we could determine the J values for most of the *p*-wave resonances, we could determine the dependence of level density on parity and also verify the $(2J+1)$ dependence of the level density. However, since it was not possible to make definite J assignments to many of the *p*-

wave resonances, we have obtained an average value for both spin states and quote a *p*-wave level spacing, D_1 , of 8.5 ± 0.6 keV and 9.2 ± 0.5 keV for ^{52}Cr and ^{54}Cr , respectively, where $1/D_1 = \rho_{1/2-} + \rho_{3/2-}$ and $1/D_0 = \rho_{1/2+}$.

From the above formula and a value of 2.9 for σ , we calculate a value of $2.67 \times (\rho_{1/2-} / \rho_{1/2+})$ for the ratio D_0/D_1 . From our experimental data the ratio D_0/D_1 is 5.3 ± 1.1 for ^{52}Cr and 6.5 ± 1.4 for ^{54}Cr . Hence, the ratio $(\rho_{1/2-} / \rho_{1/2+})$ is 2.0 ± 0.4 for ^{52}Cr and 2.4 ± 0.5 for ^{54}Cr . Even if σ were very large, these ratios would be reduced by only 11%. If we break up the energy region in intervals of about 100 keV, we find for each isotope about the same ratio in each interval as for the entire energy region. A large number of negative parity states has been reported previously for the $^{54,56,58}\text{Fe}$, $^{63,65}\text{Cu}$, and $^{66,68}\text{Zn}$ nuclides.^{6,18-20} However, the dependence of level spacing on parity for these nuclides was not as pronounced and convincing as it is in the present work. Although it cannot be claimed that no resonances in *s*- and *p*-wave level sequences have been missed and that correct parity assignments have been made to all resonances, we believe that the use of the *R*-matrix formalism of resonance analyses, the application of the Porter-Thomas law⁴ to the reduced neutron widths distributions, the use of Dyson-Mehta's statistics³ of *s*-level sequences, and the use of Bayes's theorem¹⁵ as a further check of parity assignments (as discussed in preceding sections) provide a sufficiently reliable set of resonance parameters to conclude that there is a dependence of level density on parity. If all the $l \geq 1$ resonances observed in the capture measurements of ^{52}Cr by Allen *et al.*¹¹ were assumed to be *p* wave (which would be inconsistent with the Porter-Thomas neutron width distribution as discussed earlier), there would be an even stronger parity dependence.

Soloviev²¹ has discussed theoretically the possibility of a parity dependence of level density in even-even nuclei. Camarda²² indicated a parity dependence of level density in $^{89}\text{Y} + n$ and suspected its correlation with nuclear structure. Horen *et al.*²³ pointed out the parity dependence of level density as a localized effect in the case of $^{206}\text{Pb} + n$. We conclude that level density does depend on parity for the compound nuclides ^{53}Cr and ^{55}Cr , and that nuclear structure effects are important even at high excitation energies of $6-8$ MeV.

VI. CONCLUDING REMARKS

The $^{52}\text{Cr}(n,n)$ and $^{54}\text{Cr}(n,n)$ reactions have been investigated by means of high-resolution neutron transmission measurements. Resonance parameters (E_0 , $g\Gamma_n$, and J^π) have been obtained for about 133 resonances for ^{52}Cr and 108 resonances for ^{54}Cr , which represents a considerable increase in the number of resonances studied compared with the earlier published work for these isotopes. We, therefore, have been able to provide more precise values of the average level spacings D_0 and D_1 and of the *s*- and *p*-wave strength functions for ^{52}Cr and ^{54}Cr .

On the basis of the known $(2J+1)$ dependence of level density and assuming parity independence, the ra-

tio of the average spacings for s - and p -wave resonances should be about 2.7, which is much smaller than the experimental values of 5.3 and 6.5 for these isotopes. This disagreement is larger than might be accounted for from uncertainties, such as the nonobservance of s -wave levels and the inclusion of d -wave resonances in the p -wave level sequence, and, based on the $(2J+1)$ level density law, confirms the need of parity dependence in the level density expression for ^{53}Cr and ^{55}Cr at high excitation.

ACKNOWLEDGMENTS

We would like to express our appreciation to V. K. Tikku for his assistance in the early stages of the analysis of this data. This research was sponsored by the Division of Nuclear Sciences, U.S. Department of Energy, under Contract No. DE-AC05-84OR21400 with the Martin Marietta Energy Systems, Inc., and Contract No. DE-AC02-76ER02439 with the State University of New York at Albany.

*Present address: University of Michigan, Ann Arbor, MI 48109.

¹C. Porter, H. Feshbach, and V. Weisskopf, *Phys. Rev.* **96**, 448 (1954).

²B. Block and H. Feshbach, *Ann. Phys. (N.Y.)* **23**, 47 (1963).

³F. J. Dyson, *J. Math. Phys.* **3**, 140 (1962); **3**, 157 (1962); **3**, 166 (1962); **3**, 1199 (1962); F. J. Dyson and M. L. Mehta, *ibid.* **4**, 701 (1963).

⁴C. E. Porter and R. G. Thomas, *Phys. Rev.* **104**, 483 (1956).

⁵J. R. Huizenga and L. G. Moretto, *Annu. Rev. Nucl. Sci.* **22**, 427 (1972).

⁶M. S. Pandey, J. B. Garg, and J. A. Harvey, *Phys. Rev. C* **15**, 600 (1977); **15**, 615 (1977).

⁷*Neutron Cross Section, Vol. I: Neutron Resonance Parameters and Thermal Cross Sections, Part A*, 4th ed., edited by S. F. Mughabghab, M. Divadeenam, and N. E. Holden (Academic, New York, 1981).

⁸J. B. Garg, V. K. Tikku, J. A. Harvey, R. L. Macklin, and J. Halperin, *Phys. Rev. C* **24**, 1922 (1981).

⁹R. G. Stieglitz, R. W. Hockenbury, and R. C. Block, *Nucl. Phys.* **A163**, 5912 (1971).

¹⁰H. Beer and R. R. Spencer, *Nucl. Phys.* **A240**, 29 (1975).

¹¹B. J. Allen and A. R. de L. Musgrove, in *Proceedings of the Geel Conference on Neutron Data of Structural Materials for Fast Reactors*, 1977, p. 447; see also Australian Atomic Energy Commission, Lucas Heights, Report AAEC/E-415, 1977.

¹²C. D. Bowman, E. G. Bilpuch, and H. W. Newson, *Ann. Phys. (N.Y.)* **17**, 319 (1962).

¹³M. Beer, Ph.D. thesis, State University of New York, Stony Brook, 1968.

¹⁴J. B. Garg, V. K. Tikku, and J. A. Harvey, *Phys. Rev. C* **23**, 671 (1981).

¹⁵J. B. Garg, V. K. Tikku, J. Halperin, and R. Macklin, *Phys. Rev. C* **23**, 683 (1981).

¹⁶J. A. Farrell, E. G. Bilpuch, and H. W. Newson, *Ann. Phys. (N.Y.)* **37**, 367 (1966).

¹⁷K. N. Muller and G. Rohr, *Nucl. Phys.* **A164**, 97 (1971).

¹⁸J. B. Garg, V. K. Tikku, J. A. Harvey, J. Halperin, and R. L. Macklin, *Phys. Rev. C* **25**, 1808 (1982).

¹⁹J. B. Garg, S. Jain, and J. A. Harvey, *Phys. Rev. C* **18**, 1141 (1978).

²⁰M. S. Pandey, J. B. Garg, J. A. Harvey, and W. M. Good, in *Proceedings of a Conference on Neutron Cross Sections and Technology*, Washington, D.C. Vol. 2, edited by R. A. Schrack and C. D. Bowman, U.S. Department of Commerce/National Bureau of Standards Special Publication 425, 1975, p. 748.

²¹V. G. Soloviev, Ch. Stoyanov, and A. I. Vdovin, Joint Institute of Nuclear Research, Dubna, U.S.S.R., Report P4-7499, 1973.

²²H. S. Camarda, *Phys. Rev. C* **16**, 1803 (1977).

²³D. J. Horen, J. A. Harvey, and N. W. Hill, *Phys. Rev. C* **24**, 1961 (1981).